Bioresource Technology 395 (2024) 130374

Contents lists available at ScienceDirect

Bioresource Technology

journal homepage: www.elsevier.com/locate/biortech

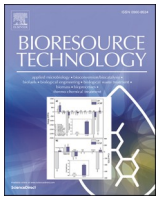

Alternating polarity as a novel strategy for building synthetic microbial communities capable of robust Electro-Methanogenesis

Shiyun Yao [a], Clifford S. Swanson [b], Zhang Cheng [a], Qiang He [b,*], Heyang Yuan [a,*]

[a] Department of Civil and Environmental Engineering, Temple University, Philadelphia, PA 19122, United States
[b] Department of Civil and Environmental Engineering, University of Tennessee, Knoxville, Knoxville, TN 37996, United States

HIGHLIGHTS

- Alternating polarity was used to build electro-methanogenic communities.
- Alternating polarity-assembled communities achieved robust biogas production.
- Alternating polarity- assembled communities showed distinct structure.
- *Methanobacterium* and *Geobacter* were dominant in the communities.
- *Methanobacterium* and *Geobacter* were highly active and interacted with each other.

ARTICLE INFO

Keywords:
Direct interspecies electron transfer
Biogas
Microbial ecology
Geobacter
Data-driven modeling

ABSTRACT

Electro-methanogenic microbial communities can produce biogas with high efficiency and have attracted extensive research interest. In this study an alternating polarity strategy was developed to build electro-methanogenic communities. In two-chamber bioelectrochemical systems amended with activated carbon, the electrode potential was alternated between +0.8 V and −0.4 V vs. standard hydrogen electrode every three days. Cumulative biogas production under alternating polarity increased from 45 L/L/kg-activated carbon after start-up to 125 L/L/kg after the 4th enrichment, significantly higher than that under intermittent cathode (−0.4 V/open circuit), continuous cathode (−0.4 V), and open circuit. The communities assembled under alternating polarity were electroactive and structurally different from those assembled under other conditions. One *Methanobacterium* population and two *Geobacter* populations were consistently abundant and active in the communities. Their 16S rRNA was up-regulated by electrode potentials. Bayesian networks inferred close associations between these populations. Overall, electro-methanogenic communities have been successfully assembled with alternating polarity.

1. Introduction

Methanogenic microbial communities are cultivated in engineered systems to convert organic wastes into methane-rich biogas (Appels et al., 2008), a renewable energy source that has attracted considerable attention (Batstone & Virdis, 2014; USDA et al., 2014). Biogas is produced cooperatively by several groups of functional microbial populations in the communities (Schink & Stams, 2013), including acetogens, syntrophs, and methanogens. The interactions of these populations can strongly affect methanogenic activity and represent one of the limiting factors for biogas production (Stams & Plugge, 2009).

Recent studies show that biogas production can be enhanced by building electro-methanogenic communities (Lovley, 2021). In addition to common fermentative bacteria, electro-methanogenic communities consist of electrotrophic methanogens and electroactive bacteria (primarily *Geobacter*) (Gao & Lu, 2021). Electrotrophic methanogens can accept extracellular electrons from cathodes and/or electroactive *Geobacter* (Cheng et al., 2009). (Rotaru et al., 2014). Compared to conventional methanogenic pathways, electro-methanogenesis is not limited by the availability and diffusion of acetate and hydrogen and thus can result in faster biogas production (Mei et al., 2018). There is continued interest in developing strategies to build electro-methanogenic communities.

Electro-methanogenic communities are conventionally assembled

* Corresponding authors.
E-mail addresses: qianghe@utk.edu (Q. He), heyang.yuan@temple.edu (H. Yuan).

https://doi.org/10.1016/j.biortech.2024.130374
Received 11 December 2023; Received in revised form 8 January 2024; Accepted 22 January 2024
Available online 26 January 2024

using cathode enrichment, microbial electrolysis, and conductive material amendment. Cathode enrichment refers to using a cathode as an electron donor to enrich electrotrophic methanogens by setting the potential at between −0.24 and −0.41 V vs. standard hydrogen electrode (SHE) (Bretschger et al., 2015). Similar to cathode enrichment, microbial electrolysis is an electrochemical process in which an external voltage is applied to drive electron transfer from the anode to the cathode (Wang et al., 2022; Zakaria & Dhar, 2019). In contrast, conductive material amendment does not impose electrochemical stimulation, but the materials act as a conduit that promotes extracellular electron transfer from electroactive bacteria to electrotrophic methanogens (Martins et al., 2018).

These conventional strategies focus on the enrichment of electrotrophic methanogens but overlook the simultaneous enrichment of electroactive bacteria. Without electroactive bacteria acting as partners to mediate electron transfer, the biogas production performance of the communities can be compromised by perturbations (Ishii et al., 2019). For example, during cathode enrichment, disconnecting the electrode for 45 min can result in a significant, irreversible decrease in biogas production (Bretschger et al., 2015). During microbial electrolysis, the electroactive bacteria enriched on the anode are unable to interact with the electrotrophic methanogens on the cathode because of the long distance between the two electrodes (Zakaria & Dhar, 2019). In addition, the cathodic potential during microbial electrolysis is often more negative than −0.41 V vs. SHE (redox potential of hydrogen evolution at pH 7) (Logan et al., 2006), leading to the enrichment of hydrogenotrophic methanogens (Wang et al., 2022). Finally, conductive materials do not create a strong driving force for building electro-methanogenic communities (Lovley, 2021), and *Geobacter*, which is by far the only electroactive bacteria involved in electro-methanogenesis (Rotaru et al., 2015), enriched with conductive materials does not necessarily contribute to electro-methanogenesis (Lovley, 2021; Mei et al., 2018; Yuan et al., 2021).

It is hypothesized that electro-methanogenic communities can be effectively assembled with alternating polarity (Fig. 1). Alternating polarity refers to switching the electrode potential periodically between cathodic and anodic potentials (Hayashi et al., 2022). When the potential is alternated, the electrode acts as a stable electron donor and acceptor for electrotrophic methanogens and electroactive bacteria, respectively. Consequently, the two populations are simultaneously enriched in a microenvironment (e.g., on conductive materials) and can interact with each other for robust electro-methanogenesis. The hypothesis is supported by previous studies (Cheng et al., 2011). One-time reversal of the electrode potential has also been reported to promote the formation of electroactive biofilm, shorten reactor start-up, and enhance methane production (Cheng et al., 2011; Li et al., 2019; Mateos et al., 2018). It should be noted that the electrode potential and alternation frequency in those studies were not precisely controlled. High alternation frequency can cause permanent damage to the electroactive biofilm (Wang et al., 2016), and the resulting communities are incapable of methanogenesis (Izadi et al., 2021; Mickol et al., 2021; Riedl et al., 2019; Yates et al., 2017). Moreover, the effects of continuous alternating polarity on the enrichment of key microbial populations and the assembly of electro-methanogenic communities have not been studied.

The goal of this study is to develop an alternating polarity strategy to build electro-methanogenic communities capable of robust biogas production. To this end, two-chamber bioelectrochemical systems were amended with granular activated carbon (Supplementary Fig. S1), and the potential of the working electrode was alternated between +0.8 and −0.4 V vs. SHE using a potentiostat. In addition to applying alternating polarity, enrichment was performed to facilitate community assembly. The electro-methanogenic activity was characterized with biochemical and electrochemical measurements, and the assembled communities were further analyzed by sequencing the 16S rRNA gene and transcript amplicons. To the best knowledge of the authors, this is the first attempt to use alternating polarity to build electro-methanogenic communities. The strategy may hold great promise in practical applications, and the assembled communities can serve as a model system to study electro-methanogenesis.

2. Materials and methods

2.1. Experimental design

Two-chamber bioelectrochemical systems were constructed as previously described (Yuan et al., 2021). Briefly, the methanogenic chamber (total volume 120 mL) was amended with 50 g of granular activated carbon and fed with 60 mL of substrate, resulting in 20 mL of headspace. A carbon brush was buried in activated carbon as the working electrode, and an Ag/AgCl reference electrode (+0.197 V vs. SHE) was installed adjacent to the working electrode. The methanogenic chamber was inoculated with digester sludge supernatant collected from a local wastewater treatment plant and fed with synthetic wastewater. The synthetic wastewater contained 3,000 mg/L fructose and 2,200 mg/L polyethylene glycol 200 as carbon sources and was slightly modified with 0.1 M phosphate buffer saline to maintain the pH. More details about the substrate composition can be found in previous studies (Yuan et al., 2021). This substrate mimics soft drink wastewater and has been shown to favor electro-methanogenesis (Mei et al., 2018; Narihiro et al., 2015). Stainless steel mesh was used as the counter electrode in another chamber. The counter-electrode chamber was filled with 0.1 M phosphate buffer saline. The two chambers were separated using a cation exchange membrane (Membrane International Inc.), and the solutions in both chambers were recirculated using a peristaltic pump at a rate of 46 mL/min. The schematic of the bioreactor can be found in Supplementary Fig. S1.

Eight bioreactors were constructed and operated in batch mode with a hydraulic retention time of three days. Duplicate bioreactors were operated under one of four conditions (Table 1): alternating polarity (+0.8 and −0.4 V vs. SHE), intermittent cathode (−0.4 V vs. SHE and

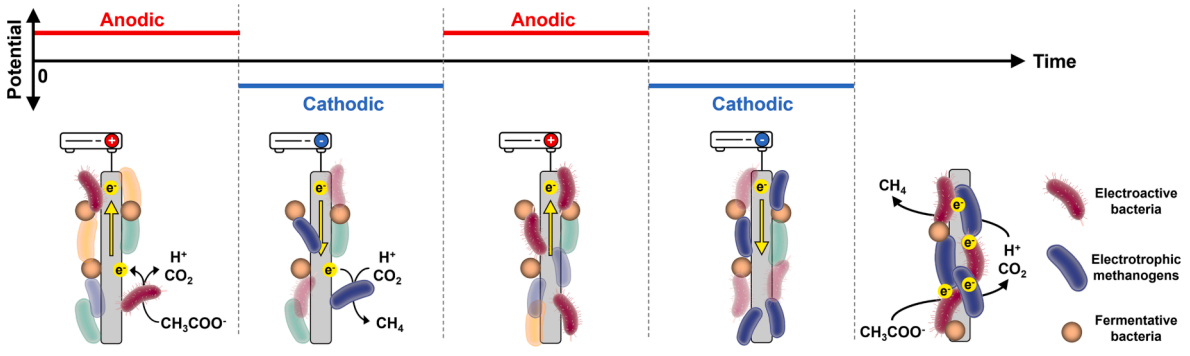

Fig. 1. Schematic of building electro-methanogenic communities with alternating polarity.

Table 1
Electrode potentials applied in the eight cycles in one enrichment. Each cycle lasted for three days.

Condition	Electrode potential (V vs. SHE)							
	Cycle 1	Cycle 2	Cycle 3	Cycle 4	Cycle 5	Cycle 6	Cycle 7	Cycle 8
Alternating	+0.8	–	−0.4	–	+0.8	–	−0.4	–
Intermittent	−0.4	–	−0.4	–	−0.4	–	−0.4	–
Continuous	−0.4	−0.4	−0.4	−0.4	−0.4	−0.4	−0.4	−0.4
Open circuit	–	–	–	–	–	–	–	–

open circuit), continuous cathode (−0.4 V vs. SHE), and open circuit. For the bioreactors operated under alternating polarity, an open-circuit cycle was performed between the cathodic and anodic cycles to promote interaction between the two populations (Wang et al., 2020). The electrode potential was poised using a multi-channel potentiostat (Squidstat^{TM} Prime, Admiral Instruments). Each condition was examined for eight cycles, and each cycle lasted three days to mitigate possible electrochemical shock. After eight cycles (24 days) of enrichment, start-up was completed, and 10% (w/w) of the activated carbon harboring electro-methanogenic communities was transferred to new bioreactors containing fresh activated carbon. The newly inoculated bioreactors were again operated under the same conditions as in the previous enrichment for eight more cycles. The enrichment was repeated four times. The schematic of the enrichment procedure can be found in Supplementary Fig. S1.

2.2. Chemical and electrochemical analyses

Biogas was collected at the end of each cycle using gas sampling bags, and the volume was measured manually using syringes and normalized to the volume of the substrate and the mass of activated carbon (L/L/kg-activated carbon). Methane content was measured using gas chromatography–mass spectrometry (8860/5977B, Agilent Co.) equipped with an Agilent CP-Molsieve 5A column (25 m X 0.25 mm) following an established method. Soluble chemical oxygen demand (COD) and pH of the effluent were measured using a standard colorimetric method (Rice et al., 2012) and a pH meter (Mettler-Toledo LLC.), respectively. Electric current was recorded using the built-in software of the potentiostat. Coulombic efficiency was calculated as previously described (Logan et al., 2006). Methane yield (Y_{CH4}) was estimated as the ratio between the number of electrons recovered as methane and the maximum number of electrons available in the removed COD:

$$Y_{CH_4} = a \bullet \left(\frac{PV_{CH_4}}{RT}\right)\left(\frac{M_{O_2}}{b \bullet \Delta COD + C}\right) \quad (1)$$

where $a = 8$ is the number of electrons transferred when carbon dioxide is reduced to methane, P is the atmospheric pressure, V_{CH4} is the volume of the methane in the produced biogas, R is the ideal gas constant, T is the temperature, $M_{O2} = 32$ is the molecular weight of oxygen, $b = 4$ is the number of electrons transferred from COD removal (ΔCOD), and C is the number of electrons transferred to/from the electrode:

$$C = \begin{cases} -\int idt, anodic \\ \int idt, cathodic \end{cases} \quad (2)$$

where i is the electrical current generated when potential is applied. At anodic potentials (positive current), the number of electrons was subtracted from the maximum number of electrons available in the removed COD because part of the electrons in the substrate were channeled to the electrode. At cathodic potentials (negative current), the number of electrons contributed by the electrode was added to the maximum number of electrons. After the last cycle of the final enrichment, cyclic voltammetry (CV) was conducted to characterize the electroactivity of the communities. Voltammograms were obtained with fresh substrate (turnover condition) at different scan rates (0.2, 1, 2, 5, 10, 20, and 50 mV/s) and a scan window of −0.4 V to +0.8 V vs. SHE, which covered the applied potentials and the redox potentials of most electroactive microbes.

2.3. Biomass collection and sequencing

Biomass samples (1.5 g of activated carbon) were collected after Cycles 7 and 8 in each enrichment. Additional biomass samples were collected from the alternating-polarity bioreactors after Cycles 5 and 6 in the 1st and 4th enrichments. Samples were stored at −80 °C prior to nucleic acid extraction. Additionally, samples for RNA extraction were stored in RNAlater stabilization solution. Genomic DNA was extracted using the MPbio FastDNA Spin kit (MP Biomedicals). RNA was extracted using the QIAGEN RNeasy PowerSoil Total RNA kit (Qiagen) followed by removal of residual DNA using the QIAGEN Dnase Max DNA-free kit (Qiagen) and reverse transcription using SuperScript IV VILO Master Mix (Thermo Fisher Scientific). DNA and cDNA samples were quality-checked and quantified using Nanodrop and the Thermo Fisher Qubit^{TM} dsDNA Quantification Assay (Thermo Fisher Scientific).

After DNA extraction, the V4 region of the 16S rRNA gene and rRNA were amplified using polymerase chain reaction (PCR) with the primer pair 515F (GTGCCAGCMGCCGCGGTAA) and 806R (GGACTACHVGGGTWTCTAAT, with unique barcodes) (Cao et al., 2021). The amplicons were quality-checked using gel electrophoresis, and amplicons with a length of 300 bp were targeted. Subsequently, the amplicons were purified with the ChargeSwitch Nucleic Acid Purification Technology (Invitrogen) and then pooled to equimolar based on the quantification results with NanoDrop ND-3300 fluorospectrometer (Thermo Fisher Scientific). The pooled library was further quantified with the KAPA Illumina Library Quantification Kit (Kapa Biosystems) and finally sequenced on an Illumina MiSeq platform (Illumina). Paired-end sequences were assembled and denoised using QIIME 2, and operational taxonomic units (OTUs) were picked using DADA2 (Callahan et al., 2016; Caporaso et al., 2010). Taxonomy was assigned using the QIIME 2 plugin feature-classifier and the SILVA database as the reference, with the classifier trained on 99% OTUs (Quast et al., 2013).

2.4. Microbial community analysis

After singletons were removed, statistical analyses were performed using the software R. These included two-sample t-test, analysis of variance (ANOVA), and Bray-Curtis dissimilarity-based principal coordinate analysis (PCoA). PCoA was performed with relative abundance (16S rRNA gene). Permutational multivariate analysis of variance (PERMANOVA) was carried out to test the significant difference of the PCoA results (N = 999). A p-value < 0.05 was used to identify a significant difference. Core populations were selected at the OTU level based on the following criteria: average relative abundance $> 0.75\%$ and occurrence $> 75\%$ across all DNA samples. A phylogenetic tree of the core populations was constructed using the software ARB and a neighbor-joining method (Ludwig et al., 2004).

Bayesian networks were constructed using the R package “bnlearn” to infer the interactions of the microbial populations (Yuan et al., 2017). Briefly, the relative abundance of 16S rRNA of the core OTUs and three key environmental factors (biogas production, cathodic current, and pH)

were combined as a single dataset and normalized to between 0 and 1:

$$v\_norm_{ij} = \frac{v_{ij} - min(v_j)}{max(v_j) - min(v_j)} \quad (3)$$

where v_norm_{ij} is the normalized variable j in sample i, v_{ij} is the observed variable j in sample i, $min(v_j)$ and $max(v_j)$ are the minimum and maximum values of variable j. The network structure was learned using a hill-climbing algorithm, and the network parameters were learned using a maximum likelihood method (Scutari, 2010). The networks were tested with leave-one-out cross validation (Bro et al., 2008). In each cross-validation cycle, the relative root-mean square error (RMSE) between the observed and predicted values was calculated:

$$RMSE = \frac{\sqrt{\frac{\sum_{i=1}^{n}(y-\hat{y})^2}{n}}}{y_{max}} \quad (4)$$

where y is the experimental value, $\hat{y}$ is the predicted value, and y_{max} is the maximum experimental value. Null model predictions were performed by manually setting the value of the node of interest (e.g., the abundance of a population or the measurement of an environmental factor) to the mean value across all samples.

3. Results and discussion

3.1. Activity of the electro-methanogenic communities

The overall activity of the microbial communities assembled with alternating polarity (+0.8/-0.4 V), intermittent cathode (−0.4 V/open circuit), continuous cathode (−0.4 V), and open circuit was characterized with bioreactor performance including biogas production, methane yield, effluent pH, and voltammetric responses. Biogas production as a key indicator of a functioning methanogenic community was expressed as cumulative biogas produced per unit volume of substrate and unit mass of activated carbon (Fig. 2A). At the end of the start-up period, alternating polarity resulted in 45 L/L/kg of biogas, which was significantly lower than the 57 L/L/kg achieved with continuous cathode (two-sample t-test, $p < 0.05$) but comparable to that obtained with intermittent cathode and open circuit. After eight cycles of enrichment, 10% of the activated carbon was used to inoculate new bioreactors containing fresh activated carbon. This enrichment procedure enhanced biogas production. The biogas produced under alternating polarity increased from 56 L/L/kg after the 1st enrichment to 65 L/L/kg and 80 L/L/kg after the 2nd and 3rd enrichments, respectively. At the end of the 4th enrichment, alternating polarity yielded 125 L/L/kg biogas and outperformed all other conditions, indicating the formation of electro-methanogenic communities that were highly efficient in biogas production.

In the 4th enrichment, the alternating-polarity bioreactors produced approximately 4 mA of anodic current (Fig. 2B), leading to an average Coulombic efficiency of 54%. This was much higher than the 5% in a previous study and indicated the high activity of electroactive bacteria (Yuan et al., 2021). The cathodic current of the alternating-polarity and intermittent-cathode bioreactors was around −0.2 mA (Fig. 2B and Supplementary Fig. S2A), whereas that of the continuous-cathode bioreactors reached up to −10 mA (Supplementary Fig. S2B). The additional electrons contributed by the cathode can explain the higher biogas production rate under continuous cathode in early enrichments (Fig. 2A). Calculations based on the average cathodic current over the eight cycles suggest that continuous cathode should theoretically result in 53 L/L/kg more biogas than alternating polarity. However, compared to alternating polarity, continuous cathode produced only slightly more biogas (10–20 L/L/kg) after the first three enrichments and 13 L/L/kg less biogas after the 4th enrichment. Using cathodic current, COD removal (Supplementary Fig. S3A), and methane content (Supplementary Fig. S3B), the methane yield of the alternating polarity-bioreactors in the 4th enrichment was estimated to be 7% (Supplementary Fig. S3C). This was significantly higher than the other bioreactors (ANOVA, $p < 0.05$), further underpinning the high efficiency of alternating polarity-assembled communities in biogas production. In line with current production, the effluent pH varied at different electrode potentials. While the effluent from the intermittent-cathode, continuous-cathode, and open-circuit bioreactors remained neutral (~7.5) throughout the enrichment, the effluent pH under alternating polarity repeatedly dropped below 6 in the first and fifth cycles when +0.8 V was applied (Supplementary Fig. S3D). Anode acidification occurs in

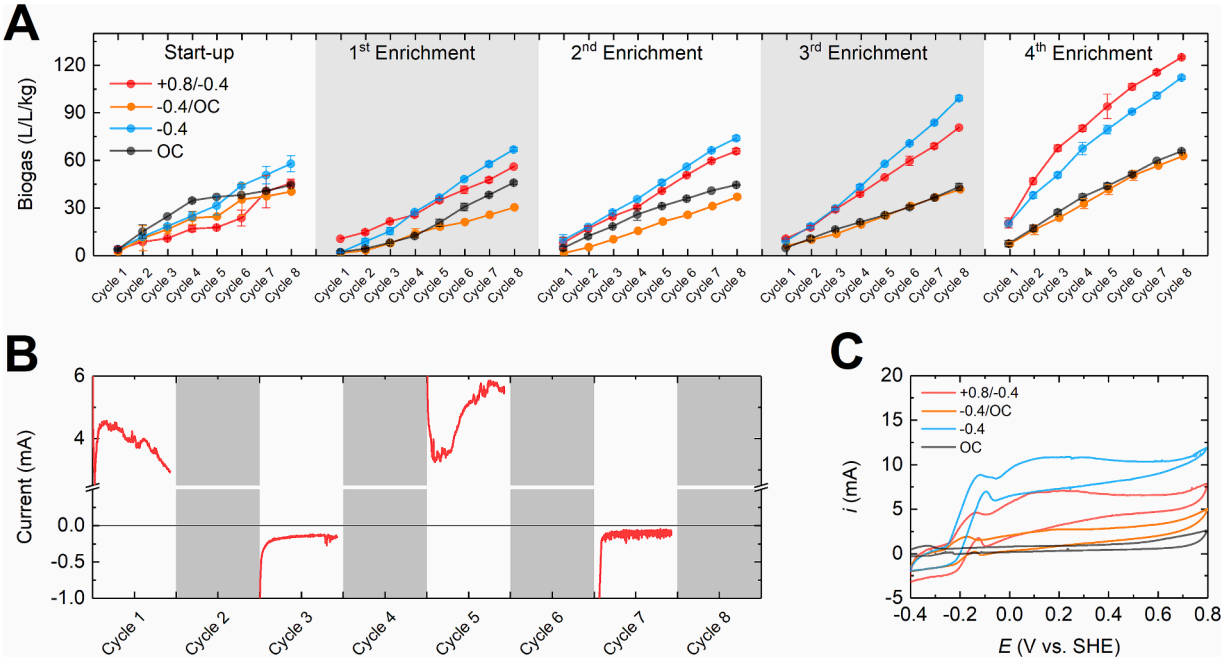

Fig. 2. (A) Cumulative biogas production during the start-up and four enrichments. (B) Current production by the alternating polarity-assembled communities in the 4th enrichment. (C) CV conducted with a scan rate of 0.2 mV/s.

bioelectrochemical systems as electroactive bacteria use the anode as an extracellular electron acceptor to oxidize organic matter to carbon dioxide and proton (He et al., 2008).

To further evaluate the electroactivity of the communities, CV was performed at a low scan rate of 0.2 mV/s (Fig. 2C). Typical sigmoidal voltammograms with peak currents were obtained with the alternating-polarity, intermittent-cathode and continuous-cathode bioreactors, suggesting the presence of redox species. In contrast, no peak currents were observed in the voltammogram of the open-circuit bioreactors. Using the first derivative of the voltammograms, the redox potentials of the species were estimated to be −0.2 V and 0 V vs. SHE (Supplementary Fig. S2C). These were more positive than the redox potential of carbon dioxide reduction to methane at pH 7 (−0.24 V vs. SHE) and were consistent with typical redox potentials of electroactive *Geobacter* (Richter et al., 2009). CV was further performed with the scan rate ranging from 1 to 50 mV/s. The peak current in the voltammograms was found to be strongly correlated with the square root of the scan rate ($R^2 > 0.98$, Supplementary Fig. S2D), implying a reversible and diffusion-controlled electron transfer process (Bard & Faulkner, 1980). The results collectively confirmed the electroactivity of the electro-methanogenic communities assembled with electrode potentials.

3.2. Dynamics of the electro-methanogenic communities

The effects of electrode potential and enrichment on microbial community dynamics were studied using Bray-Curtis dissimilarity-based PCoA. As shown in Fig. 3A, communities assembled under different conditions still overlapped after start-up. This indicates that electrode potential alone may not act as a strong driving force for microbial community assembly. However, combining electrode potential and enrichment significantly changed the community structure. For example, the communities from alternating polarity started to shift since the 1st enrichment and reached the lower left corner after the 4th enrichment (Fig. 3B). Communities assembled under other conditions also shifted but toward different directions (Fig. 3C–E), resulting in clusters that were clearly separated from those in the alternating-polarity bioreactors at the end of the 4th enrichment (Fig. 3A). Overall, the results show successful assembly of distinct electro-methanogenic communities with alternating polarity.

A detailed examination of community dynamics over enrichment suggests that alternating polarity may be a more reliable approach for building electro-methanogenic communities. In particular, the communities in the duplicate alternating-polarity bioreactors shifted in a synchronized manner as the enrichment proceeded (Fig. 3B). The communities in the duplicate open-circuit bioreactors also clustered closely after each enrichment (Fig. 3C), which was expected as the enrichment procedure did not represent a strong perturbation. In contrast, intermittent and continuous cathodes caused noticeable divergence in community structure. The two communities in the duplicate intermittent-cathode bioreactors evolved along different trajectories and were distant from each other after the 4th enrichment (Fig. 3D). A similar differentiation was observed for the communities in the continuous-cathode bioreactors (Fig. 3E). The difference in community dynamics under different conditions highlights the important role of the anodic potential (+0.8 V) in building stable electro-methanogenic communities. This may be achieved through the enrichment of electroactive bacteria, which serve as alternative electron-donating partners and help maintain the community structure under perturbations.

3.3. Core populations in the electro-methanogenic communities

OTUs with an average relative abundance greater than 0.75% and present in more than 75% of the DNA samples were defined as core populations (Yuan et al., 2019). Based on this criterion, 22 core populations were selected (Fig. 4), accounting for 63% of the total relative abundance. The core populations could be further divided into three guilds potentially responsible for distinct functions: methanogens, *Geobacter*, and fermentative bacteria.

Two methanogens were identified as core populations: OTU1998 and OTU2011. OTU1998 was phylogenetically close to *Methanobacterium formicicum* and had a high relative abundance of 5−10% during start-up and early enrichments in all bioreactors (Supplementary Fig. S4). As the enrichment proceeded, its abundance was maintained at about 5% under alternating polarity but dropped below 1% under other conditions (ANOVA, $p < 0.05$) (Fig. 4). This result was consistent with the findings of a previous study (Yuan et al., 2021), in which anodic potentials were applied (0 V and +0.4 V vs. SHE) to enrich electroactive bacteria but high abundances of three *Methanobacterium*-related populations were observed. Several *Methanobacterium* spp. have been observed as dominant methanogens in bioelectrochemical systems and have been speculated to perform extracellular electron uptake from both electroactive bacteria and cathodes (Mayer et al., 2019). The higher abundance of OTU1998 in the presence of anodic potentials than at intermittent and continuous cathodic potentials may result from its interactions with anode-enriched bacteria. The other methanogen, OTU2011, belonged to the genus *Methanobrevibacter*. Its relative abundance remained stable at about 1% under different conditions (Supplementary Fig. S4) and was slightly higher in the alternating-polarity bioreactors than in other bioreactors in the 4th enrichment (ANOVA, $p < 0.05$) (Fig. 4). *Methanobrevibacter* spp. are hydrogenotrophic and ubiquitous in various environments (Poehlein et al., 2017), but their electrotrophic activity has not been documented.

Two *Geobacter*-related OTUs, OTU1634 and OTU1635, were among

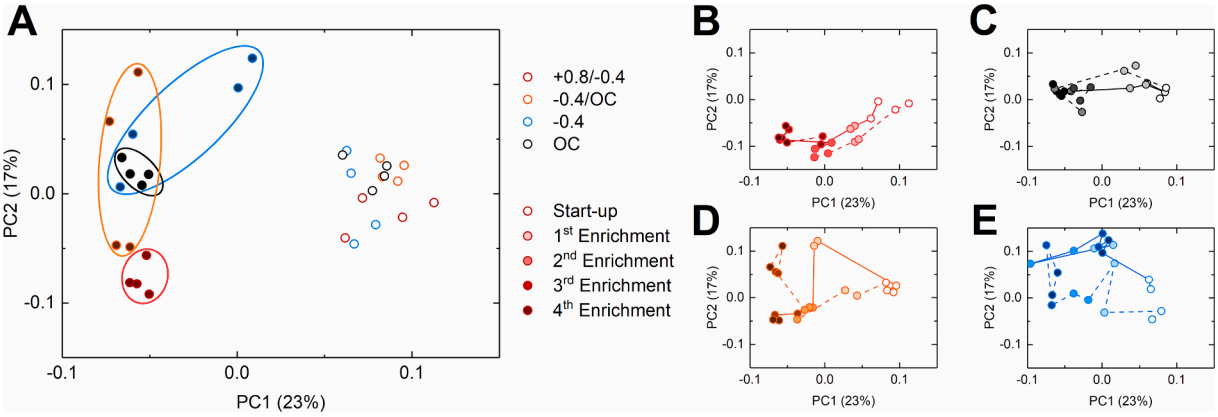

Fig. 3. Bray-Curtis dissimilarity-based PCoA. (A) Difference in community strucutre after start-up and 4th enrichment. Community dynamics under (B) alternating polarity, (C) open circuit, (D) intermittent, and (E) cathode continuous cathode. Darker colors indicate later enrichments.

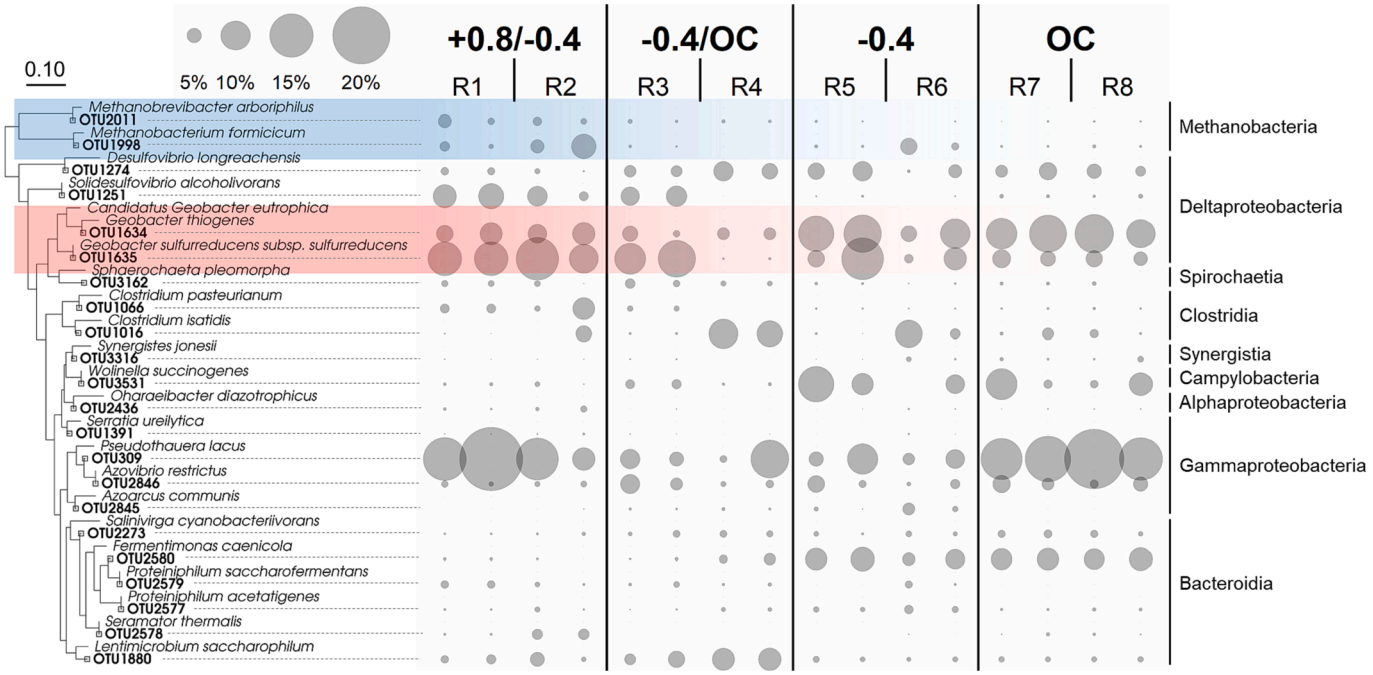

Fig. 4. Phylogenetic tree and relative abundance of the 22 core OTUs in the 4th enrichment. The four samples under each condition were collected from duplicate bioreactors after Cycles 7 and 8.

the dominant populations throughout the enrichment (Supplementary Fig. S4). The enrichment of OTU1634 appeared to be less efficient with electrode potentials than under open circuit. In the 4th enrichment, the relative abundance of OTU1634 was 4–7% in the presence of anodic and/or cathodic potentials but reached 12% in the open-circuit bioreactors, making it the second most abundant population (Fig. 4). OTU1634 shares 97% similarity with *Candidatus* Geobacter *eutrophica*, a novel *Geobacter* species discovered in a previous study (Mei et al., 2018). Electrochemical stimulation and omics analysis revealed *Ca.* G. *eutrophica*'s capability of extracellular electron transfer to electrodes and methanogens (Yuan et al., 2021). *Geobacter*-related OTU1634 may carry similar metabolic pathways, and its lower abundance under alternating polarity implies its low growth efficiency with the anode as an electron acceptor. In contrast, the anode favored the enrichment of the other *Geobacter*, OTU1635. Its abundance was consistently higher than 8% under alternating polarity (Supplementary Fig. S4) and increased to 12% in the 4th enrichment (Fig. 4), significantly higher than the 6% under other conditions (ANOVA, $p < 0.05$). With 100% similarity to *Geobacter sulfurreducens*, a model species for extracellular electron transfer (Logan et al., 2019), OTU1635 was very likely electroactive. However, *G. sulfurreducens* is not known to donate electrons to methanogens, and therefore the involvement of *Geobacter*-related OTU1635 in electro-methanogenesis remains an open question.

In addition to methanogens and *Geobacter*, the communities assembled with alternating polarity were also dominated by three fermentative bacteria from the families Clostridiaceae, Desulfovibrionaceae, and Rhodocyclaceae. Among them, *Clostridium*-related OTU1066 was highly abundant (18%) in the 1st enrichment (Supplementary Fig. S4). Based on its high similarity to *Clostridium pasteurianum* (100%), OTU1066 was likely responsible for converting carbohydrates into short-chain volatile fatty acids, ethanol, and hydrogen (Biebl, 2001). This population was gradually replaced by *Solidesulfovibrio*-related OTU1251 and *Pseudothauera*-related OTU309, whose abundances in the 4th enrichment were 7% and 15%, respectively (Fig. 4). The change in their abundance may result from interactions among these fermentative bacteria, *Geobacter*, and methanogens. It is possible that *Solidesulfovibrio*, *Pseudothauera*, and *Geobacter* cooperate and compete with *Clostridium* for organic carbon. In the presence of an anode and methanogens as electron acceptors, the growth of *Geobacter* is promoted, resulting in high abundances of the associated *Solidesulfovibrio* and *Pseudothauera*. The detailed ecology in the electro-methanogenic communities warrants further investigation. In comparison, the communities assembled with intermittent and continuous cathodes showed a much less defined structure without significantly dominant populations (i.e., many populations with low abundances) (Supplementary Fig. S4).

3.4. Growth activity and interactions of the core populations

The growth activity of the core populations was characterized with 16S rRNA transcript profiling. With an average 16S rRNA transcript abundance of 3% across all samples, *Methanobacterium*-related OTU1998 was identified as one of the most active populations (Supplementary Fig. S5). Its growth was significantly stimulated by alternating polarity than by other conditions (ANOVA, $p < 0.05$). Under alternating polarity, OTU1998 became progressively more active over enrichment (Fig. 5A), and the expression of its 16S rRNA was consistently up-regulated when electrode potentials were applied (Fig. 5B). For example, during start-up, its transcript abundance at the anodic and cathodic potentials was 0.2 and 1.4 folds relative to that at open circuit, respectively. These numbers increased to 0.5 and 3.1 folds in the 4th enrichment. The growth activity of OTU1998 in the presence of an anode is consistent with previous findings and may be a result of its interaction with electron-donating partners (Yuan et al., 2021). Meanwhile, the up-regulation of its 16S rRNA expression by the cathodic potential can serve as evidence of OTU1998's ability to accept extracellular electrons from the electrode.

Geobacter-related OTU1634 and OTU1635 had the highest transcript abundance in most of the samples (Supplementary Fig. S5). OTU1634 was particularly active under alternating polarity and open circuit, showing a transcript abundance of 9% at the end of the enrichment under those conditions (Fig. 5A). This population responded to electrochemical stimulation in a similar manner to the methanogen. In the 4th enrichment, the anodic and cathodic potentials caused a 1.3-fold and 2.2-fold increase in transcript abundance, respectively, compared to open circuit (Fig. 5B). The 16S rRNA expression of OTU1635 was also more active when the electrode potentials were applied but showed an

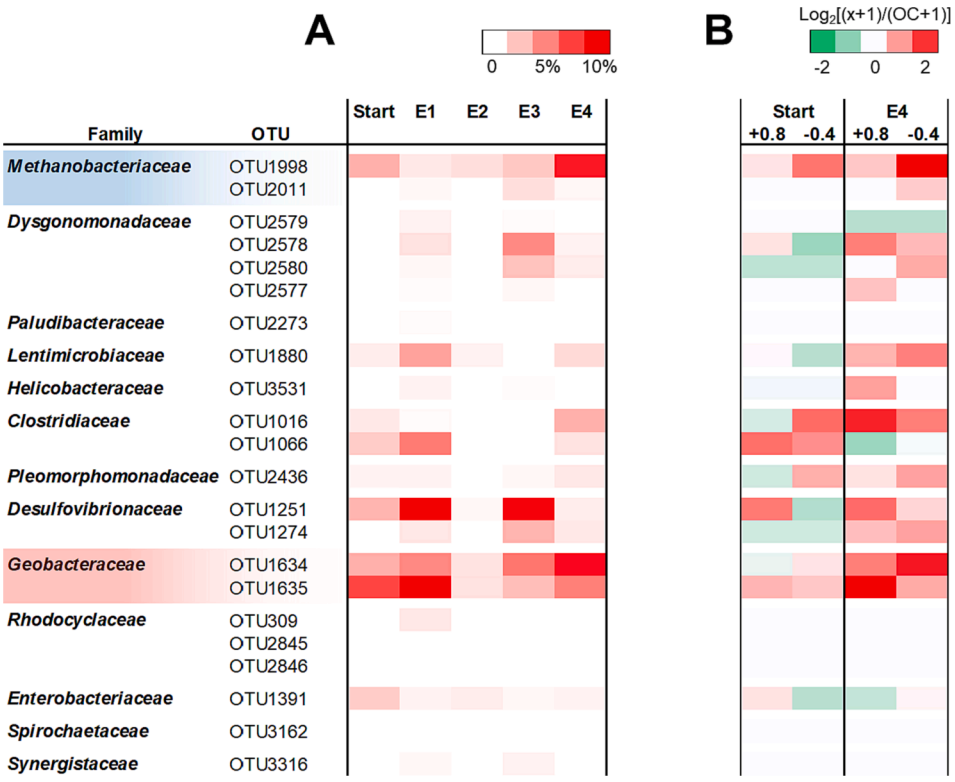

Fig. 5. (A) Growth activity (16S rRNA transcript abundance) of the 22 core populations under alternating polarity. (B) Relative growth activity (growth activity at the anodic and cathodic potentials relative to that at open circuit) during start-up and in the 4th enrichment.

opposite trend. Specifically, in the 4th enrichment, the transcript abundance at the anodic potential was 3.2 folds relative to that at open circuit, whereas the change at the cathodic potential was only 0.9 folds (Fig. 5B). The high growth activity of OTU1634 and OTU1635 demonstrates their electroactivity and importance in electro-methanogenic communities, but the different electrochemical responses are indicative of their different roles in the communities.

To further understand the interactions between the *Methanobacterium* and *Geobacter* populations, Bayesian networks were constructed with the core populations and three environmental factors (biogas production, pH, and cathodic current) that showed electrode potential-dependent variation. Bayesian networks are probabilistic graphical models capable of inferring the causal relationships between variables via directed acyclic graphs. The networks inferred that OTU1998 could be affected by ten parent nodes (Fig. 6A). Among them, OTU1634 had the highest positive network parameter (0.42) followed by OTU1066 (0.14) and OTU1635 (0.09). The cathodic current was inferred to exert a slightly negative impact on OTU1998 (network parameter −0.06). Using the actual values of the ten nodes, the abundance of OTU1998 was predicted with an R^2 of 0.72 and an RMSE of 7.8% (Fig. 6B). Considering that the prediction was performed at the OTU level, the accuracy was acceptable compared to previous studies

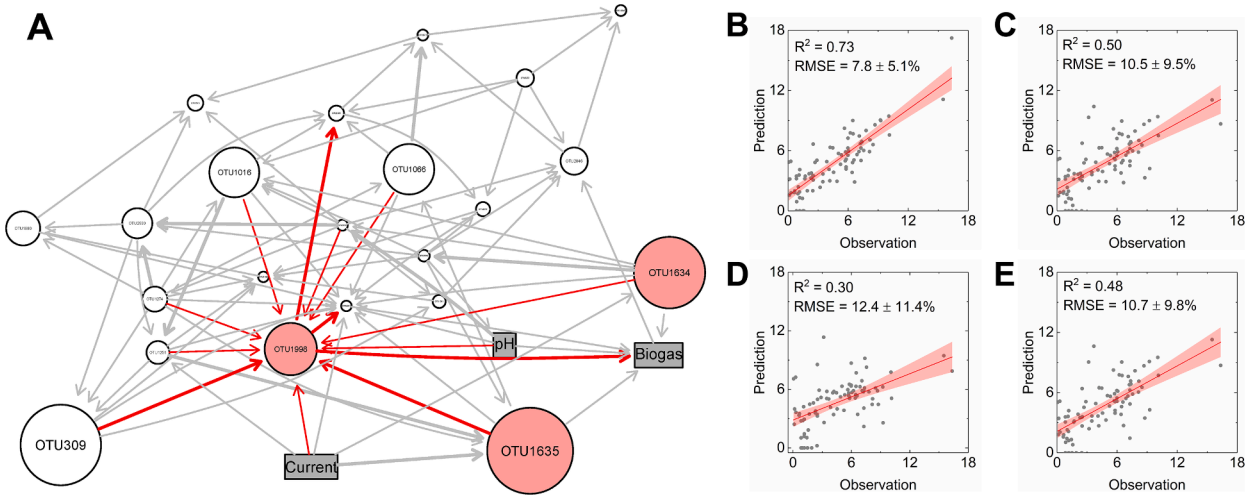

Fig. 6. (A) Bayesian network constructed with the core populations (circle nodes) and three environmental factors (rectangular nodes). The size of the circle nodes represents the average abundance across all samples. Methanogens and Geobacter are highlighted in red. Prediction of the abundance of Methanobacterium-related OTU1998 was performed with (B) the actual values of all nodes, (C) the mean value of electric current and the actual values of all other nodes, (D) the mean abundance of OTU1634 and the actual values of all other nodes, (E) the mean abundance of OTU1635 and the actual values of all other nodes.

(Yuan et al., 2017). Null predictions were performed to reveal the influence of cathodic current, OTU1634, and OTU1635 on OTU1998 in a more quantitative manner. When the mean values of these nodes were fed into the networks, the predictions became noticeably less accurate (Fig. 6C–E). Particularly, the R^2 and RMSE of the null prediction with OTU1634 dropped to 0.30 and 12.4%, respectively, underpinning the close relationship between this *Geobacter* population and the methanogen.

3.5. Perspectives

Electro-methanogenic microbial communities have attracted extensive interest due to their high efficiency in biogas production (Cheng et al., 2009; Rotaru et al., 2014; Zakaria & Dhar, 2019). Significant efforts have been made to build electro-methanogenic communities in engineered systems to improve biogas production (Gao et al., 2021; Martins et al., 2018; Wang et al., 2022). The communities assembled with conventional strategies are susceptible to perturbations (Bretschger et al., 2015; Ishii et al., 2019). The unstable performance can be attributed to the absence of electroactive bacteria, key electron-donating partners of electrotrophic methanogens (Yuan et al., 2021). Based on previous studies (Cheng et al., 2011; Li et al., 2019; Mateos et al., 2018), it was hypothesized that electroactive bacteria and electrotrophic methanogens could be simultaneously enriched with alternating polarity (Fig. 1), resulting in electro-methanogenic communities capable of robust biogas production. The findings of the present study collectively support the hypothesis. At the end of the enrichment, the cumulative biogas produced under alternating polarity was 11% higher than that under continuous cathode and 50% higher than that under open circuit (Fig. 2). The communities assembled with alternating polarity were structurally different from those under other conditions (Fig. 3).

The alternating polarity strategy can have important environmental implications. For example, after community assembly, activated carbon harboring electro-methanogenic communities can be added in full-scale systems to enhance biogas production. Despite the great potential, the energy efficiency and system stability of such a strategy are largely unknown. At the community assembly stage, the application of alternating polarity consumes energy. On the other hand, after successful assembly, the communities are expected to actively perform electro-methanogenesis without the need for continuous energy input. This is supported by the biogas production performance in the open circuit cycle under alternating polarity (Fig. 2A), as well as the high abundance and active interactions of *Geobacter* and methanogens (Figs. 4–6). In the absence of electrode potential, the community structure and electro-methanogenic activity can be adversely affected by microbial immigrants from the influent (Frigon & Wells, 2019), and alternating polarity may need to be applied for a short period of time to rebuild the community. The trade-off between the energy consumption for building and maintaining electro-methanogenic communities and the energy gain from enhanced biogas production remains to be systematically investigated.

In addition to practical applications, electro-methanogenic communities assembled with alternating polarity may serve as a model system to provide insight into the ecophysiology of electrotrophic methanogens. The high abundance and activity of the putative electrotrophic methanogen OTU1998 at the anodic and cathodic potentials (Figs. 4 & 5, Supplementary Figs S4 & S5) are in agreement with previous findings (Gao et al., 2021; Zheng et al., 2020), demonstrating the ability of some of the *Methanobacterium* spp. to accept electrons from both electrodes and electroactive bacteria. However, the metabolic pathways involved in extracellular electron uptake from the two electron donors remain elusive. In a previous study, multiple copies of the *mvhB* gene were found in the genomes of *Methanobacterium* spp. and were more actively expressed under electrochemical stimulation. The *mvhB*-encoded iron-rich polyferredoxins may be used to shuttle extracellular electrons to the heterodisulfide reductase/[NiFe]–hydrogenase complex for flavin-based electron bifurcation and methanogenesis (Watanabe & Shima, 2021).

Electro-methanogenic communities assembled with alternating polarity may also help us understand the ecophysiology of electroactive *Geobacter*. The *Geobacter* spp. observed in this study are likely to be involved in both electro-methanogenesis and hydrogenotrophic methanogenesis. Particularly, OTU1634 is phylogenetically related to *Ca.* G. *eutrophica* and may be capable of hydrogen production (Mei et al., 2018; Yuan et al., 2021). This speculation is supported by the observation of biogas production in the anodic cycle under alternating polarity (Fig. 2) when most of the extracellular electrons are channeled to the electrode (Coulombic efficiency 54%). The strong association between *Methanobacterium*-related OTU1998 and *Ca.* G. *eutrophica*-related OTU1634 inferred with Bayesian network analysis (Fig. 6D) may also result from the involvement of both electro-methanogenesis and interspecies hydrogen transfer. Such metabolic versatility is, in principle, advantageous as it allows the two partners to cope with perturbations (e.g., absence of both anode and cathode), thereby outcompeting other populations and dominating the community.

Although alternating polarity has been proven promising in this study, the electrode potential and alternation frequency remain to be optimized. In particular, the anodic potential can have a strong impact on the community structure (Torres et al., 2009). While the effect of anodic potential on electro-methanogenic communities is still inconclusive, it may be more favorable to apply lower anodic potentials (e.g., +0.2 V vs. SHE) in the case of alternating polarity. A moderate anodic potential allows some of the extracellular electrons to be channeled to electrotrophic methanogens during the enrichment of electroactive bacteria (Yuan et al., 2021), thus maintaining the electro-methanogenic activity of the communities. The effect of electrode potential can be more complicated when alternation frequency (e.g., 10 min or 2 h) is considered. Limited evidence suggests that high frequency does not favor the assembly of electro-methanogenic communities (Riedl et al., 2019; Yates et al., 2017). It is possible that the alternation frequency should be longer than the doubling time of the populations to be enriched so that they have sufficient time to adapt to the electrochemical stimulation (Izadi et al., 2021; Mickol et al., 2021). The entangled effects of electrode potential and alternation frequency on community structure and microbial activity need to be better understood for more efficient assembly of electro-methanogenic communities.

4. Conclusions

In this study, an alternating polarity strategy was developed to build electro-methanogenic communities capable of robust biogas production. The communities assembled with alternating polarity outperformed the communities assembled with intermittent cathode, continuous cathode, and open circuit in terms of biogas production. The communities assembled with alternating polarity were structurally different from those assembled under other conditions and were dominated by one *Methanobacterium* population and two *Geobacter* populations. These populations were highly active under alternating polarity. Data-driven modeling was performed to infer their association.

CRediT authorship contribution statement

Shiyun Yao: Writing – original draft, Formal analysis, Data curation. **Zhang Cheng:** Formal analysis, Data curation. **Qiang He:** Writing – review & editing, Supervision, Project administration, Formal analysis, Conceptualization. **Heyang Yuan:** Writing – review & editing, Writing – original draft, Supervision, Project administration, Funding acquisition, Formal analysis, Conceptualization.

Declaration of competing interest

The authors declare that they have no known competing financial interests or personal relationships that could have appeared to influence the work reported in this paper.

Data availability

Data will be made available on request.

Acknowledgments

This work was supported by the National Science Foundation [CBET-2128365], the Summer Research Award at Temple University, and the Global Energy Ecosystems (GE^2) Research Development Program of the Office of Research, Innovation & Economic Development at the University of Tennessee, Knoxville.

Appendix A. Supplementary data

Supplementary data to this article can be found online at https://doi.org/10.1016/j.biortech.2024.130374.

References

Appels, L., Baeyens, J., Degrève, J., Dewil, R., 2008. Principles and potential of the anaerobic digestion of waste-activated sludge. Prog. Energy Combust. Sci. 34 (6), 755–781.
Bard, A.J., Faulkner, L.R., 1980. Electrochemical methods: fundamentals and applications. Wiley, New York.
Batstone, D.J., Virdis, B., 2014. The role of anaerobic digestion in the emerging energy economy. Curr. Opin. Biotechnol. 27, 142–149.
Biebl, H., 2001. Fermentation of glycerol by Clostridium pasteurianum—batch and continuous culture studies. J. Ind. Microbiol. Biotechnol. 27 (1), 18–26.
Bretschger, O., Carpenter, K., Phan, T., Suzuki, S., Ishii, S.I., Grossi-Soyster, E., Flynn, M., Hogan, J., 2015. Functional and taxonomic dynamics of an electricity-consuming methane-producing microbial community. Bioresour. Technol. 195, 254–264.
Bro, R., Kjeldahl, K., Smilde, A., Kiers, H., 2008. Cross-validation of component models: a critical look at current methods. Anal. Bioanal. Chem. 390 (5), 1241–1251.
Callahan, B.J., McMurdie, P.J., Rosen, M.J., Han, A.W., Johnson, A.J.A., Holmes, S.P., 2016. DADA2: High-resolution sample inference from Illumina amplicon data. Nat. Methods 13, 581.
Cao, L., Yang, L., Swanson, C.S., Li, S., He, Q., 2021. Comparative analysis of impact of human occupancy on indoor microbiomes. Front. Environ. Sci. Eng. 15, 1–10.
Caporaso, J.G., Kuczynski, J., Stombaugh, J., Bittinger, K., Bushman, F.D., Costello, E.K., Fierer, N., Peña, A.G., Goodrich, J.K., Gordon, J.I., 2010. QIIME allows analysis of high-throughput community sequencing data. Nat. Methods 7 (5), 335–336.
Cheng, K.Y., Ho, G., Cord-Ruwisch, R., 2011. Novel methanogenic rotatable bioelectrochemical system operated with polarity inversion. Environ. Sci. Tech. 45 (2), 796–802.
Cheng, S., Xing, D., Call, D.F., Logan, B.E., 2009. Direct biological conversion of electrical current into methane by electromethanogenesis. Environ. Sci. Tech. 43 (10), 3953–3958.
Frigon, D., Wells, G., 2019. Microbial immigration in wastewater treatment systems: analytical considerations and process implications. Curr. Opin. Biotechnol. 57, 151–159.
Gao, K., Lu, Y., 2021. Putative extracellular electron transfer in methanogenic archaea. Front. Microbiol. 12, 611739.
Gao, K., Wang, X., Huang, J., Xia, X., Lu, Y., 2021. Response of methanogen communities to the elevation of cathode potentials in bioelectrochemical reactors amended with magnetite. Appl. Environ. Microbiol. 87 (21), e01488–e01521.
Hayashi, K., Griffin, J., Harper, K.C., Kawamata, Y., Baran, P.S., 2022. Chemoselective (Hetero) arene electroreduction enabled by rapid alternating polarity. J. Am. Chem. Soc. 144 (13), 5762–5768.
He, Z., Huang, Y., Manohar, A.K., Mansfeld, F., 2008. Effect of electrolyte pH on the rate of the anodic and cathodic reactions in an air-cathode microbial fuel cell. Bioelectrochemistry 74 (1), 78–82.
Ishii, S.I., Imachi, H., Kawano, K., Murai, D., Ogawara, M., Uemastu, K., Nealson, K.H., Inagaki, F., 2019. Bioelectrochemical stimulation of electromethanogenesis at a seawater-based subsurface aquifer in a natural gas field. Front. Energy Res. 6, 144.
Izadi, P., Gey, M.N., Schlüter, N., Schröder, U., 2021. Bidirectional electroactive microbial biofilms and the role of biogenic sulfur in charge storage and release. Iscience 24 (8), 102822.
Li, Z., Fu, Q., Kobayashi, H., Xiao, S., Li, J., Zhang, L., Liao, Q., Zhu, X., 2019. Polarity reversal facilitates the development of biocathodes in microbial electrosynthesis systems for biogas production. Int. J. Hydrogen Energy 44 (48), 26226–26236.
Logan, B.E., Hamelers, B., Rozendal, R., Schröder, U., Keller, J., Freguia, S., Aelterman, P., Verstraete, W., Rabaey, K., 2006. Microbial fuel cells: methodology and technology. Environ. Sci. Tech. 40 (17), 5181–5192.
Logan, B.E., Rossi, R., Ragab, A.A., Saikaly, P.E., 2019. Electroactive microorganisms in bioelectrochemical systems. Nat. Rev. Microbiol. 17 (5), 307–319.
Lovley, D.R., 2021. Electrotrophy: other microbial species, iron, and electrodes as electron donors for microbial respirations. Bioresour. Technol. 126553.
Ludwig, W., Strunk, O., Westram, R., Richter, L., Meier, H., Yadhukumar Buchner, A., Lai, T., Steppi, S., Jobb, G., Förster, W., Brettske, I., Gerber, S., Ginhart, A.W., Gross, O., Grumann, S., Hermann, S., Jost, R., König, A., Liss, T., Lüßmann, R., May, M., Nonhoff, B., Reichel, B., Strehlow, R., Stamatakis, A., Stuckmann, N., Vilbig, A., Lenke, M., Ludwig, T., Bode, A., Schleifer, K.H., 2004. ARB: a software environment for sequence data. Nucleic Acids Res. 32 (4), 1363–1371.
Martins, G., Salvador, A.F., Pereira, L., Alves, M.M., 2018. Methane Production and Conductive Materials: A Critical Review. Environmental Science & Technology.
Mateos, R., Sotres, A., Alonso, R.M., Escapa, A., Morán, A., 2018. Impact of the start-up process on the microbial communities in biocathodes for electrosynthesis. Bioelectrochemistry 121, 27–37.
Mayer, F., Enzmann, F., Lopez, A.M., Holtmann, D., 2019. Performance of different methanogenic species for the microbial electrosynthesis of methane from carbon dioxide. Bioresour. Technol. 289, 121706.
Mei, R., Nobu, M.K., Narihiro, T., Yu, J., Sathyagal, A., Willman, E., Liu, W.-T., 2018. Novel Geobacter species and diverse methanogens contribute to enhanced methane production in media-added methanogenic reactors. Water Res. 147, 403–412.
Mickol, R.L., Eddie, B.J., Malanoski, A.P., Yates, M.D., Tender, L.M., Glaven, S.M., 2021. Metagenomic and metatranscriptomic characterization of a microbial community that catalyzes both energy-generating and energy-storing electrode reactions. Appl. Environ. Microbiol. 87 (24), e01676–e01721.
Narihiro, T., Kim, N.-K., Mei, R., Nobu, M.K., Liu, W.-T., 2015. Microbial community analysis of anaerobic reactors treating soft drink wastewater. PLoS One 10 (3), e0119131.
Poehlein, A., Daniel, R., Seedorf, H. 2017. The draft genome of the non-host-associated methanobrevibacter arboriphilus strain dh1 encodes a large repertoire of adhesin-like proteins. *Archaea*, **2017**.
Quast, C., Pruesse, E., Yilmaz, P., Gerken, J., Schweer, T., Yarza, P., Peplies, J., Glöckner, F.O., 2013. The SILVA ribosomal RNA gene database project: improved data processing and web-based tools. Nucleic Acids Res. 41 (D1), D590–D596.
Rice, E.W., Bridgewater, L., Association, A.P.H., 2012. Standard methods for the examination of water and wastewater. American public health association Washington, DC.
Richter, H., Nevin, K.P., Jia, H., Lowy, D.A., Lovley, D.R., Tender, L.M., 2009. Cyclic voltammetry of biofilms of wild type and mutant Geobacter sulfurreducens on fuel cell anodes indicates possible roles of OmcB, OmcZ, type IV pili, and protons in extracellular electron transfer. Energ. Environ. Sci. 2 (5), 506–516.
Riedl, S., Brown, R.K., Alvarez Esquivel, D.Y., Wichmann, H., Huber, K.J., Bunk, B., Overmann, J., Schröder, U., 2019. Cultivating electrochemically active biofilms at continuously changing electrode potentials. ChemElectroChem 6 (8), 2238–2247.
Rotaru, A.-E., Shrestha, P.M., Liu, F., Shrestha, M., Shrestha, D., Embree, M., Zengler, K., Wardman, C., Nevin, K.P., Lovley, D.R., 2014. A new model for electron flow during anaerobic digestion: direct interspecies electron transfer to Methanosaeta for the reduction of carbon dioxide to methane. Energ. Environ. Sci. 7 (1), 408–415.
Rotaru, A.-E., Woodard, T.L., Nevin, K.P., Lovley, D.R., 2015. Link between capacity for current production and syntrophic growth in Geobacter species. Front. Microbiol. 6 (744).
Schink, B., Stams, A.J., 2013. Syntrophism among prokaryotes. The prokaryotes, Springer, in, pp. 471–493.
Scutari, M., 2010. Learning bayesian networks with the bnlearn R package. journal of statistical software. J. Stat. Softw. 35 (3), 1–22.
Stams, A.J., Plugge, C.M., 2009. Electron transfer in syntrophic communities of anaerobic bacteria and archaea. Nat. Rev. Microbiol. 7 (8), 568–577.
Torres, C.S.I., Krajmalnik-Brown, R., Parameswaran, P., Marcus, A.K., Wanger, G., Gorby, Y.A., Rittmann, B.E., 2009. Selecting anode-respiring bacteria based on anode potential: phylogenetic, electrochemical, and microscopic characterization. Environ. Sci. Tech. 43 (24), 9519–9524.
USDA, DOE, USEPA. 2014. Biogas Opportunities Roadmap.
Wang, B., Liu, W., Zhang, Y., Wang, A., 2020. Intermittent electro field regulated mutualistic interspecies electron transfer away from the electrodes for bioenergy recovery from wastewater. Water Res. 185, 116238.
Wang, X.-T., Zhang, Y.-F., Wang, B., Wang, S., Xing, X., Xu, X.-J., Liu, W.-Z., Ren, N.-Q., Lee, D.-J., Chen, C., 2022. Enhancement of methane production from waste activated sludge using hybrid microbial electrolysis cells-anaerobic digestion (MEC-AD) process – a review. Bioresour. Technol. 346, 126641.
Wang, X., Zhou, L., Lu, L., Lobo, F.L., Li, N., Wang, H., Park, J., Ren, Z.J., 2016. Alternating current influences anaerobic electroactive biofilm activity. Environ. Sci. Tech. 50 (17), 9169–9176.
Watanabe, T., Shima, S., 2021. MvhB-type polyferredoxin as an electron-transfer chain in putative redox-enzyme complexes. Chem. Lett. 50 (2), 353–360.
Yates, M.D., Ma, L., Sack, J., Golden, J.P., Strycharz-Glaven, S.M., Yates, S.R., Tender, L. M., 2017. Microbial electrochemical energy storage and recovery in a combined electrotrophic and electrogenic biofilm. Environ. Sci. Technol. Lett. 4 (9), 374–379.
Yuan, H., Sun, S., Abu-Reesh, I.M., Badgley, B.D., He, Z., 2017. Unravelling and reconstructing the nexus of salinity, electricity, and microbial ecology for bioelectrochemical desalination. Environ. Sci. Tech. 51 (21), 12672–12682.
Yuan, H., Mei, R., Liao, J., Liu, W.-T., 2019. Nexus of stochastic and deterministic processes on microbial community assembly in biological systems. Front. Microbiol. 10 (1536), 1536.

Yuan, H., Wang, X., Lin, T.-Y., Kim, J., Liu, W.-T., 2021. Disentangling the syntrophic electron transfer mechanisms of Candidatus geobacter eutrophica through electrochemical stimulation and machine learning. Sci. Rep. 11 (1), 15140.

Zakaria, B.S., Dhar, B.R., 2019. Progress towards catalyzing electro-methanogenesis in anaerobic digestion process: Fundamentals, process optimization, design and scale-up considerations. Bioresour. Technol. 121738.

Zheng, S., Liu, F., Wang, B., Zhang, Y., Lovley, D.R., 2020. Methanobacterium Capable of Direct Interspecies Electron Transfer. Environ. Sci. Tech. 54 (23), 15347–15354.